Original Article

High Performance Polymers

High Performance Polymers
2015, Vol. 27(3) 274–287

DOI: 10.1177/0954008314545137
hip.sagepub.com
SAGE

Dynamic mechanical and dielectric relaxation studies of chlorobutyl elastomer nanocomposites: Effect of nanographite loading and temperature

S. K. Tiwari[1], R. N. P. Choudhary[2] and S. P. Mahapatra[1]

Abstract

Primary and secondary relaxation behavior of chlorobutyl elastomer nanocomposites have been studied as a function of variation in nanographite loading in the temperature range from -100°C to $+100^{\circ}$C and in the frequency range of 100–10^6 Hz respectively. The effect of nanographite loadings on glass transition temperature was marginal for all the composites in the narrow range of -10°C to 10°C. The nonlinearity in tan δ and storage modulus has been explained on the concept of filler–polymer interaction and aggregation of nanographites. The effect of variation in nanographite loadings on the dielectric relaxation such as complex and real parts of impedance was distinctly visible. The electric modulus formalism has been utilized to further investigate the conductivity and relaxation phenomenon. The frequency dependence of electrical conductivity has been investigated using percolation theory. The phenomenon of percolation in the composites has been discussed based on the measured changes in electrical conductivity. The percolation threshold as studied by electrical conductivity occurred in the vicinity of 4–6 phr of nanographite loading. Cole–Cole, Nyquist plots, and Argand diagram confirm the existence of non-Debye/nonlinear relationship. Scanning electron microscopic images show agglomeration of the nanographite and formation of a continuous network structure.

Keywords

Relaxation, nanocomposites, dynamic mechanical, dielectric, conductivity, percolation

Introduction

Many materials used in our daily life are composites, which are often made up of at least two constituents or phases. The outstanding mechanical properties of many composites, especially the unique combination of low density with high strength and stiffness, have led not only to extensive research but also to highly developed technologies.[1,2] Conductive polymer composites have received considerable attention due to their technological importance in a wide variety of applications such as electrostatic charge dissipation material in pressure-sensitive sensors, transducers, electromagnetic interference shielding material and as packaging material in electronics, aircraft, and telecommunications. They are also used as antistatic materials in low-temperature heaters, energy storage devices such as batteries, fuel cells, and supercapacitors, and hybrid power sources. Normally, the conductivity in a polymer is imparted by incorporation of electrically conductive fillers into the polymer matrix. Metal fillers,[3] carbon fibers,[4] and conductive carbon black[5] have been used in practice. Carbon blacks and silica have been traditionally used as reinforcing materials in elastomers. But recently much attention is being focused on the applicability of novel carbon-based fillers like carbon silica, dual phase fillers,[6] carbon nanotubes (CNTs),[7] and nanographite.[8] Graphite is composed of layered nanosheets with good electrical conductivity of 10^4 S/cm at room temperature. Normally in graphite, three sp^2 hybrid orbitals (each containing one electron) are formed from the 2s and two of the 2p orbitals of each carbon atom and participate in covalent bonding

[1] Department of Chemistry, National Institute of Technology, Raipur, Chhattisgarh, India
[2] Department of Physics, Institute of Technical Education & Research (ITER), Siksha O Anusandhan University (SOA) University, Bhubaneswar, Odisha, India

Corresponding author:
S. P. Mahapatra, Department of Chemistry, National Institute of Technology, G. E. Road, Raipur 492010, Chhattisgarh, India.
Email: om_spm@yahoo.com

Figure 1. TEM image of 4 phr nanographite-reinforced chlorobutyl elastomer nanocomposite. TEM: transmission electron microscopic.

with three surrounding carbon atoms in the graphite planes. The fourth electron is located in the remaining 2p orbital, which projects above and below the graphite plane, to form part of a poly aromatic *p*-system. Delocalization of electrons in *p*-electron system is the cause of high stability and electrical conductivity. The important properties of chlorobutyl rubber (CIIR) that makes it a superior elastomer in various industrial and automotive applications are its low gas and moisture permeability, good weathering resistance, and high thermal stability. Although there have been many studies on the effect of addition of nanographite in polymer matrix, it hasn't been reported in chlorobutyl elastomer matrix. Relaxation in filled elastomers is time, temperature, frequency, and strain dependent. Processing variables (i.e. the type of filler, volume fraction of filler in the composite, the extent of interactions of filler with the polymer matrix, etc.) and operating variables (i.e. strain amplitude, strain rate, frequency, and temperature of testing) have a significant effect on the dynamic properties of the polymers. Dynamic mechanical analysis of polymer composites is an important tool to study the viscoelastic behavior of the material for evaluation of its use in various engineering applications.

The present study deals with the primary dynamic mechanical and secondary dielectric relaxation spectra of chlorobutyl elastomer nanocomposites in the temperature range from -100°C to $+100^{\circ}$C and in the frequency range of 100–10^6 Hz respectively, as a function of nanographite loading. The effects of variation in nanographite loading and temperature on dynamic mechanical properties like loss tangent (tan δ), storage modulus (ε') and loss modulus (ε'') have been reported. The effects of variation in nanographite loading on dielectric characteristics like dissipation factor (loss tangent), real and complex parts of impedance, dielectric permittivity, and conductivity have been also studied. Additionally the data obtained were also analyzed by dielectric modulus formalism. Percolation threshold of multiwalled CNTs (MWCNTs) loading in chlorobutyl matrix as obtained from electrical conductivity and dielectric permittivity measurement has also been found.

Table 1. Formulation of unfilled and nanographite-reinforced chlorobutyl elastomer nanocomposites.[a]

Ingredient	CNC1	CNC2	CNC3	CNC4	CNC5
CIIR	100	100	100	100	100
Nanographite (phr)	0	2	4	6	8

CIIR: chlorobutyl rubber; CNC: CIIR nanocomposite; ZnO: zinc oxide; TMTD: tetramethylthiuram disulfide.
[a]Each mix contains ZnO (5 phr), stearic acid (2 phr), TMTD (1 phr), and sulfur (1.5 phr).

Experimental

Materials

Cholorobutyl elastomer (1.25% chlorine content, Mooney viscosity ML_{1+8}at 100°C = 38) was procured from Bayer AG (Germany). Nanographite of 95% was purchased from Iljin (Korea). Prior to use, the nanographite was treated with acid mixture under ultrasonication to remove amorphous carbon and metallic impurities. Step I: 1 g of nanographite was bath sonicated in 500 ml 6 M nitric acid (HNO_3) for 4 h and was diluted with distilled water and cooled to room temperature. Then, it was filtered on a 0.22 μm Millipore polycarbonate membrane and rinsed with distilled water until the pH value of the filtrate was neutral. Finally, a thick paper-like material was peeled off from the filter membrane and dried at 120°C in vacuum overnight. This procedure is a pretreatment process because it can only remove the unreacted catalyst. The obtained material was used as the initial material for the following procedures. Step II: The above treated nanographite was refluxed in 500 ml 6 M HNO_3 at 120°C for 4 h, a reaction temperature of 120°C. Then, the mixture was diluted with distilled water and cooled to room temperature. Finally, the same filtering and drying procedure as employed for step I was followed to get pure and oxidized nanographite. The presence of oxygen increases polymer–filler interactions due to the formation of complex physicochemical bonds between the filler surface and polymer matrix. Increased filler loading leads to increase in polymer–filler interactions thereby making a portion of the polymer matrix attached to the filler surface.[9] The adsorption of polymer layers to the graphite surfaces and distribution of nanographite in chlorobutyl matrix is shown in Figure 1. Zinc oxide was chemically pure grade and had a specific gravity of 5.4. Tetramethylthiuram disulfide was supplied by ICI Ltd (Rishra, Hooghly, West Bengal, India) having a specific gravity of 1.42. Other compounding ingredients like sulfur and stearic acid were of chemically pure grade procured from standard suppliers.

Sample preparation

The rubber was compounded with the ingredients according to the formulations of the mixes (Table 1). Compounding

was done in a Brabender plastograph at 60 r/min followed by laboratory size (325 × 150 mm^2) two-roll mixing mill at a friction ratio of 1:1.25 according to ASTM D 3182 standards while carefully controlling the temperature, nip gap, time of mixing, and uniform cutting operation. The temperature range for mixing was 65–70°C. After mixing, the elastomer compositions were molded in an electrically heated Moore hydraulic press using molding conditions determined by Monsanto rheometer (R-100; St Louis, Missouri, USA) according to ASTM D2084 and ASTM D5289 procedures.

Testing

Dynamic mechanical properties. Dynamic mechanical properties were obtained using a dynamic mechanical testing analyzer(TA Instruments, New Castle, Delaware, USA) over a temperature range of −100 to 100°C, at a frequency of 1 Hz, and at 1% strain.

Dielectric relaxation spectra. The dielectric and electrical properties of chlorobutyl elastomer nanocomposites were obtained using a computer-controlled impedance analyzer (LCR meter) Hioki-3532-50 LCR Hi tester (Japan) on application of an alternating electric field across the sample cell with an aluminum foil (blocking electrode) in the frequency range of 10^2–10^6 Hz. The parameters like dielectric permittivity (ε') and dielectric loss tangent (tan δ) were obtained as a function of frequency. The electrical conductivity (σ) was calculated from the dielectric data using the relation:

$$\sigma_{ac} = \omega \varepsilon_0 \varepsilon' \tan \delta \quad (1)$$

where ω is $2\pi f$ (f is frequency), ε_0 is permittivity of a vacuum and ε' is dielectric constant or relative permittivity and is calculated by expression:

$$\varepsilon' = \frac{C_p}{C_0} \quad (2)$$

where C_p is the observed capacitance of the sample and C_0 is the vacuum capacitance of the cell and is calculated using the expression:

$$C_0 = \frac{\varepsilon_0 A}{d} \quad (3)$$

where A is area of the sample, d is thickness of the sample, and tan δ is the dielectric loss. Real and imaginary parts of impedance (Z' and Z'') have been calculated using the following relations, respectively.

$$Z' = Z \cos\theta \quad (4)$$

$$Z'' = Z \sin\theta \quad (5)$$

Where Z is measured impedance and θ is measured phase angle.

Scanning electron microscopy. Morphology of the compounds has been studied using an INCA Penta FETX3-8113 scanning electron microscope. Prior to scanning electron microscopic (SEM) studies, the surface of the samples was sputter coated with gold. The fractured surfaces from tensile test were also studied. SEM images of cholorobutyl elastomer nanocomposites at increasing nanographite concentration have been shown in Figure 2. The figure shows good distribution of nanographite in the chlorobutyl matrix.

Results and discussion

Dynamic mechanical analysis

Effect of temperature on loss tangent. Figure 3 shows the loss tangent spectra of CIIR composites reinforced with increasing amounts of nanographite as a function of temperature. From Figure 3 it can be observed that the location of maximum value of loss tangent (tan δ_{max}) is not significantly affected by the extent of nanographite loading. All the samples show the glass transition in the narrow temperature range from −10°C to 10°C. This can be explained on the basis of relaxation dynamics of the polymer matrix. One of the main features of reinforced elastomer is that majority of polymer chains are in contact with the filler surfaces. Addition of filler into the polymer matrix induces a gradient of glass transition temperature (T_g) in the polymer chains that are in the vicinity of the fillers due to the existence of strong dynamical heterogeneities.[10,11] When a polymer is cooled through the glass transition region, the physical properties of the polymer in the nonequilibrium state (at temperature lower than T_g), such as volume and enthalpy, gradually recover to new equilibrium values through the configurationally rearrangement of polymer segments. The rate of the rearrangement or relaxation process depends on the local environment surrounding the relaxation entities and hence reflects the extent of environmental restriction on those entities. But increasing filler loading shows decrease in the magnitude of the loss tangent with simultaneous broadening of the peak. The influence of filler on the damping behavior of filled polymer systems can be explained by two possible factors. One is a decrease in free volume that limits the mobility of molecular chains, usually in case of elastomeric polymers, so that the damping value decreases. The other factor is an internal friction between the fillers and polymer chains and between the filler particles themselves over the transition range, which increases with temperature, thereby causing greater movement of molecular chains so that the damping ability increases.[12]

Effect of temperature on ε' and ε''. The variation in storage modulus (ε') as a function of temperature (−100 to 100°C) is shown in Figure 4. Irrespective of the nanographite loadings all the curves show characteristic sigmoid variation of ε' with temperature. The higher value of ε' with

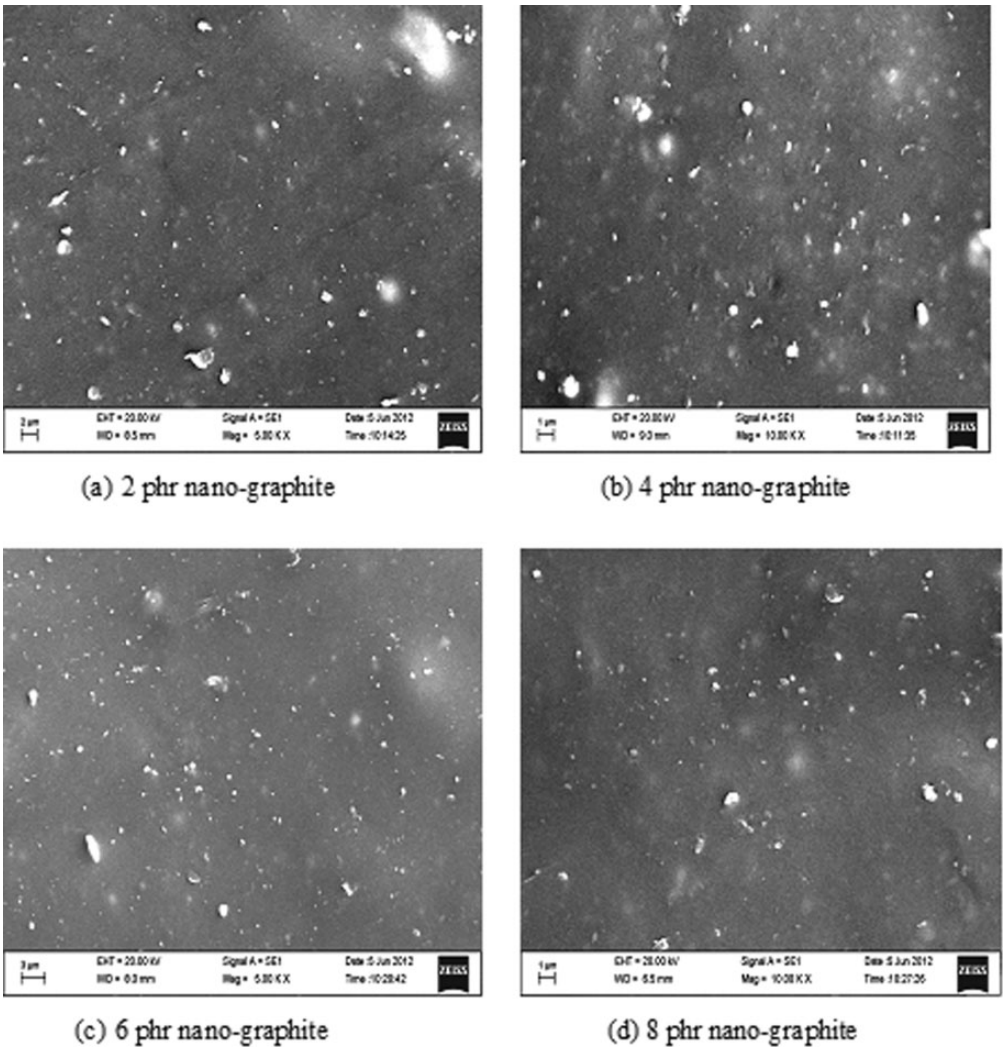

Figure 2. State of dispersion of nanographite in chlorobutyl elastomer: (a) 2 phr; (b) 4 phr; (c) 6 phr; and (d) 8 phr nanographite loading.

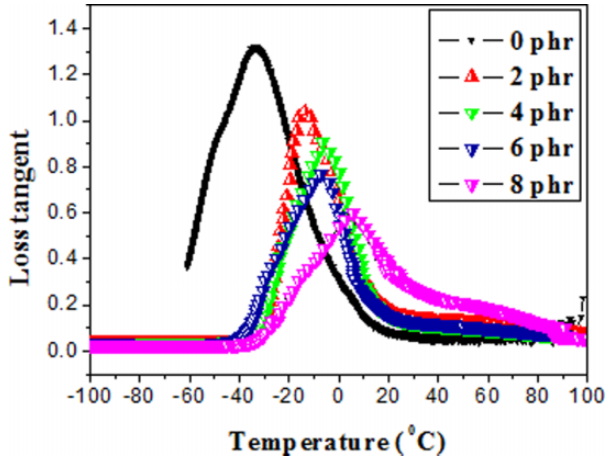

Figure 3. Variation of tan δ with temperature in chlorobutyl elastomer nanocomposites: effect of nanographite loadings. tan δ: loss tangent.

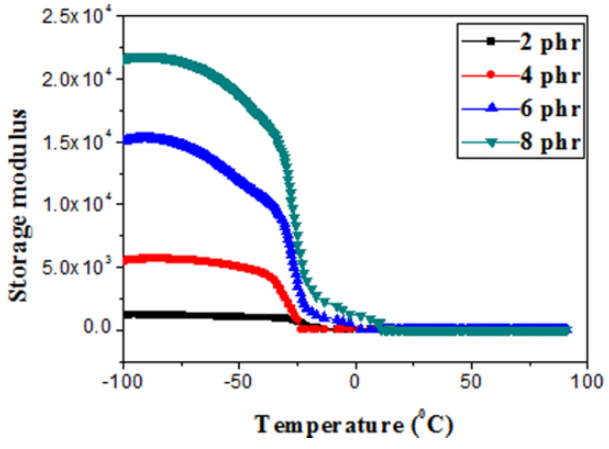

Figure 4. Variation of ε' with temperature in chlorobutyl elastomer nanocomposites: effect of nanographite loadings. ε': storage modulus.

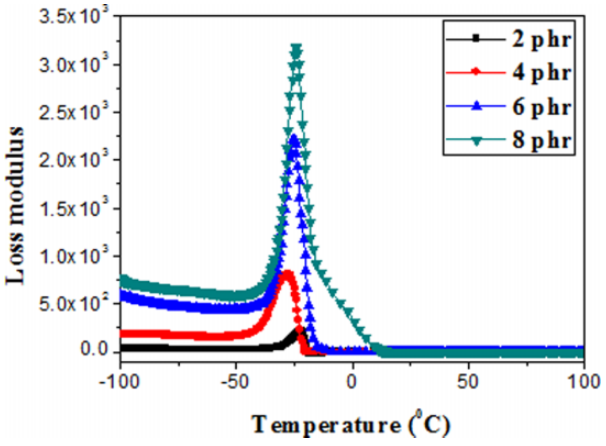

Figure 5. Variation of ε'' with temperature in chlorobutyl elastomer nanocomposites: effect of nanographite loadings. ε'': loss modulus.

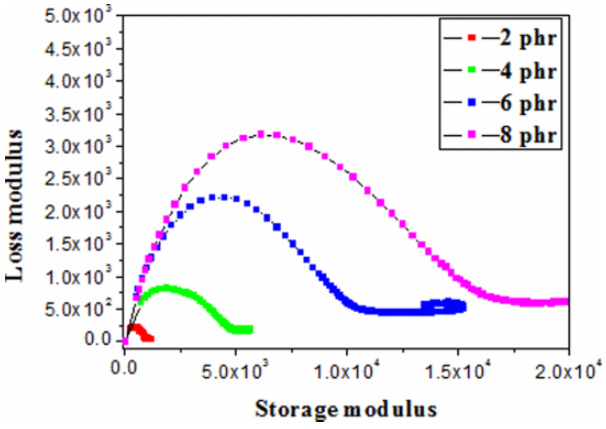

Figure 6. Cole–Cole plots of chlorobutyl elastomer nanocomposites at increasing nanographite loadings.

increase in nanographite loading is due to formation of more filler network and also because of the decrease in volume content of base polymer. The effect of incorporation of a filler on the mechanical properties of elastomeric materials can be partially explained as follows: if particles of high elastic modulus are dispersed through a low elastic modulus matrix, it is obvious that the modulus of the mixture will be higher than that of the matrix, solely because of the decrease in volume content of matrix substance. However, for a filler to be really reinforcing in nature, many other factors come into the picture, the most important being the force of adhesion of the matrix to the particle surface which plays a crucial role. The temperature dependence of ε'' for various nanographite loadings is shown in Figure 5. A distinct transition peak at $-25°C$ may be attributed to the motion of methyl group directly attached to the backbone of CIIR. Incorporation of nanographite has some effect on the location and intensity, but the amount of nanographite does not affect the temperature at

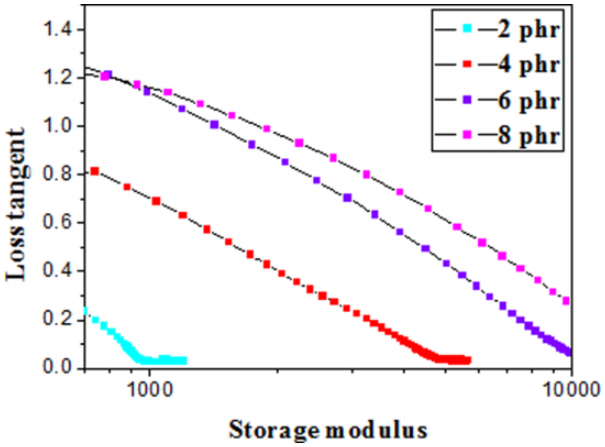

Figure 7. Plots of tan δ versus ε' of chlorobutyl elastomer nanocomposites at increasing nanographite loadings. tan δ: loss tangent; ε': storage modulus.

peak; however, the intensity slightly increases with filler loadings. Higher filler loadings result in a percolated network of filler particles that can influence relaxation on a different scale.[9] The percolation effect is usually considered to be effective for relaxation of longer time scales, such as terminal relaxation observed in some rheological measurements.[13]

Cole–Cole plots. The relaxation dynamics can also be expressed in terms of Cole–Cole plots, that is, relationship between ε' and ε''. Cole–Cole plots for nanographite-reinforced chlorobutyl composites are shown in Figure 6. Irrespective of nanographite loading at all concentrations of the filler, the usual depressed semicircle can be observed which clearly indicates the presence of a reinforcing element. The large change observed on the arc radius in the Cole–Cole plot indicates the relaxation dynamics and a significant alteration of chain conformation due to nanographite interaction.[14] Irrespective of MWCNT concentrations, smooth arcs are observed with no humps indicating good dispersion of MWNT in CIIR matrix.

Relationship between tan δ and ε'. Dynamic mechanical properties of polymeric system may show different types of dependence with one another, especially when fillers are incorporated. A linear relationship between tan δ and log E' was also established by Namboodiri for carbon black-filled ethylene propylene diene monomer vulcanizates. Figure 7 shows the plot of tan δ as a function of log E' with variation of nanographite loading. The linear nature of the plot could be mathematically expressed as:

$$\tan\delta = m\log E' + C \tag{6}$$

where m is the slope of the line and C is a constant.

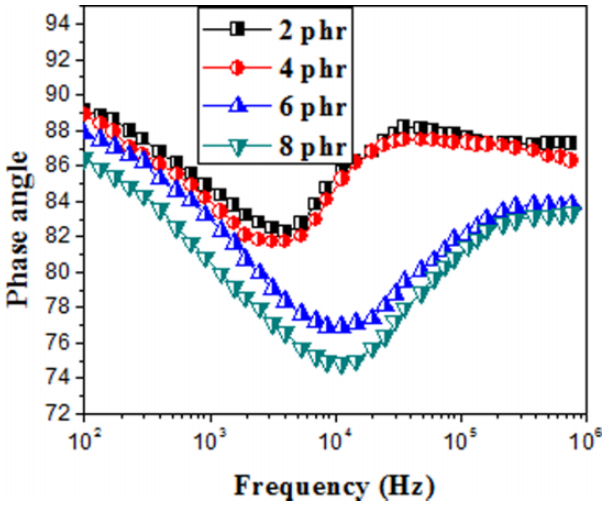

Figure 8. Variation of phase angle with frequency in chlorobutyl elastomer nanocomposites at increasing nanographite loadings.

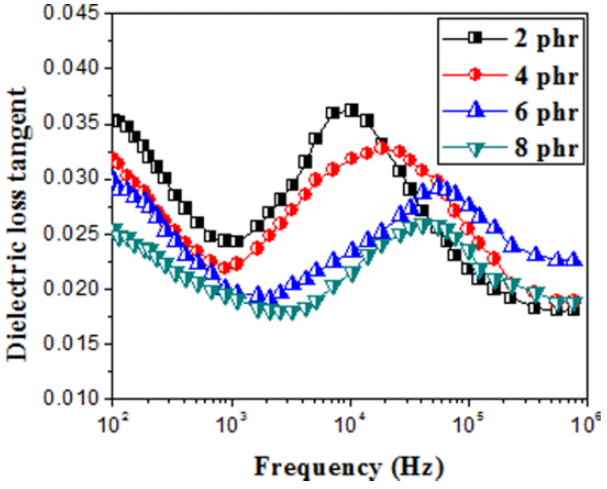

Figure 9. Variation of dielectric tan δ with frequency in chlorobutyl elastomer nanocomposites at increasing nanographite loadings. tan δ: loss tangent.

Dielectric relaxation spectra

Phase angle. Figure 8 shows the variation of phase angle with frequency at increasing nanographite loadings. From the figure it can be observed that irrespective of amount of nanographite in the composite, at low frequencies the value of phase angle is close to 88°–90°. But with increase in frequency there is a decrease in phase angle and reaches a peak in the range of 5×10^3 Hz at low nanographite loadings (2 and 4 phr), as at low frequencies the value of phase angle corresponds to resistive characteristics [$Z \approx R$]. But with increase in frequency there is a decrease in phase angle and reaches a peak in the range of 10^4 Hz at higher loadings (6 and 8 phr). It can also be observed that as nanographite loading increases the minimum phase angle reaches about 75° which corresponds to capacitors [$Z \approx 1/j(2\pi fC)$].[9]

Table 2. Bound rubber content as a function of nanographite loading in chlorobutyl elastomer nanocomposites for different solvents after 15 days.

Nanographite concentration (phr)	Trichloroethylene	Chloroform	Benzene
2	40.2	49	56
4	47.8	53	61
6	49.2	57	65.8
8	52	59.5	67.6

Dielectric tan δ. Figure 9 shows the variation in dielectric tan δ as a function of frequency for different nanographite loadings. From the figure it can be observed that irrespective of nanographite loading there is a gradual decrease followed by an increasing trend in tan δ values with frequency. In the accessible frequency range, the spectrum exhibits one relaxation peak for each nanographite loading. It is observed that the value of tan δ is due to the reduction of chain mobility in the amorphous phase. The peaks shift systematically toward higher frequencies with increase in nanographite loading. The broadening of peak indicates the spread of relaxation time with different mean time constants, hence a non-Debye type of relaxation in materials is observed. The dielectric relaxation behavior of a polymer composite mainly depends upon the distribution of filler particles in the polymer matrix. Incorporation of fillers like nanographite results in hydrodynamic as well as complex physicochemical interactions between polymer matrix and the filler surface. With increase in nanographite loading, the maximum tan δ shifted toward higher frequency, that is, 1×10^4 Hz for 2 phr to 7×10^4 Hz for 6 phr. This increase in frequency can be explained on the basis of the mechanical and viscoelastic properties of cross-linked and reinforced multiphase polymeric materials. Addition of functional fillers results in not only hydrodynamic interactions but also leads to complex physicochemical interactions between the polymer matrix and the filler surface.[15,16] These elastomer–filler interactions are often characterized by the content of the apparent 'bound' rubber, which is determined as the amount of insoluble rubber adhering to the dispersed filler before vulcanization. Since the amount of bound rubber (shown in Table 2) is related to the filler loading it can be regarded as a measure of the interactions between the filler and matrix.[17]

Impedance analysis

Real part of complex impedance. Figure 10 shows variation of real part of complex impedance (Z') as a function of frequency at increasing nanographite loadings. Irrespective of the nanographite concentrations, Z' shows a monotonous

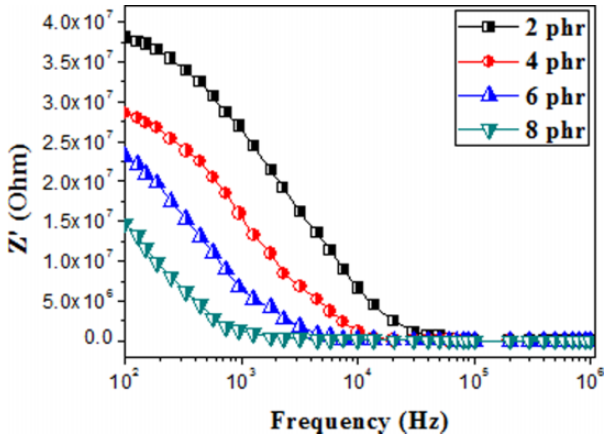

Figure 10. Z' as a function of frequency of chlorobutyl elastomer nanocomposites: effect of nanographite loadings. Z': real part of impedance.

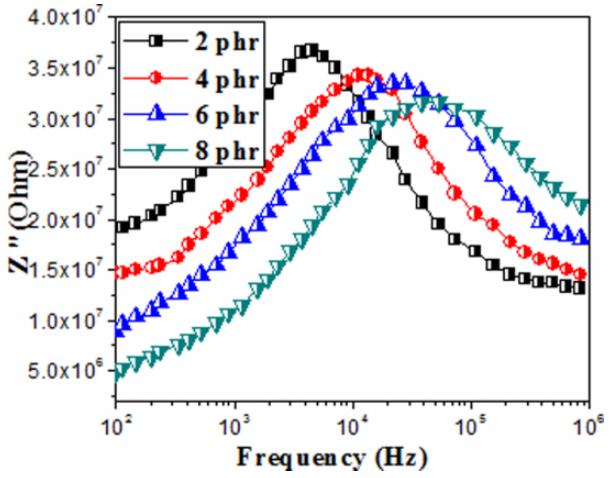

Figure 11. Z'' as a function of frequency of chlorobutyl elastomer nanocomposites: effect of nanographite loadings. Z'': imaginary part of impedance.

decrease with increasing frequency and curves almost merge for all nanographite loadings in the higher frequency region (>10^5 *Hz*). However, in the low frequency region, Z' value is gradually decreasing with nanographite loading. The decrease in Z' with nanographite loading and frequency indicates the possibility of increasing electrical conductivity with nanographite loading and frequency (a more detailed study of alternating current (AC) conductivity is given in subsequent sections of the manuscript). The merging of Z' curves in the higher frequency region may be attributed to the release of space charge.

Imaginary part of complex impedance. Figure 11 represents the variation of imaginary part of complex impedance (Z'') with frequency. The impedance loss spectra have features such as decrease in the height of the peak and shift in peak toward higher frequencies (10^3–10^4 Hz) with increasing

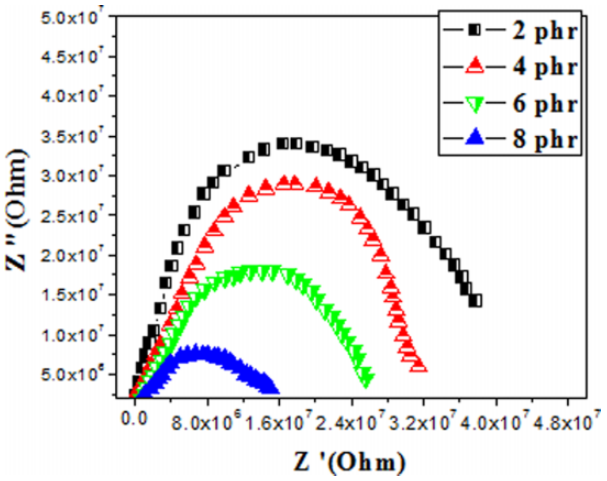

Figure 12. Nyquist plots of chlorobutyl elastomer nanocomposites: effect of nanographite loadings.

nanographite concentrations. This confirms better capacitive nature and decrease in resistance of the composites with nanographite loading. This increase in frequency can be explained on the basis of the mechanical and viscoelastic properties of cross-linked and reinforced multiphase polymeric materials. The addition of the filler particles has a significant effect on the dielectric behavior of the sample. Filler particles in the matrix acquire induction charges in the presence of the applied external field; polarization effects take place in the so called Maxwell–Wagner–Sillar's polarizations. Below the critical concentration of the filler loading, the interparticle distance is large enough so that neighboring local fields apparently do not interact. Thus, dielectric factor in this region increases slowly. But as the filler loading increases, the Maxwell–Wagner–Sillar's effect increases due to reduction in the interaggregate distance giving rise to dielectric properties. The Z'' data hve been fitted to different spectral functions commonly used such as Debye, Cole–Cole, Cole–Davidson, Havriliak–Negami, and Frohlich.[18] The best fit was obtained using a Havriliak–Negami function, superimposed with Frohlic function to account the effect of conductivity. The spectral function $Z''(\omega)$ can be expressed as:

$$Z''(\omega) = Z''(\omega)_{\mathrm{HN}} + Z''(\omega)_{\mathrm{Fr}} + \frac{\theta\sigma}{\omega} \qquad (7)$$

where $Z''(\omega)_{\mathrm{HN}}$ denotes Havriliak–Negami function form and $Z''(\omega)_{\mathrm{Fr}}$ denotes Frohlic function, ω denotes the angular frequency, σ is the direct current (DC) conductivity, and θ is a constant.

Nyquist plots. Figure 12 shows the Nyquist plot, that is, the relationship between imaginary part of impedance (Z'') and real part of impedance (Z') of chlorobutyl elastomer nanocomposites as a function of increasing nanographite concentration. It can be observed that increasing nanographite

Table 3. Bulk resistance (from Figure 12) of chlorobutyl elastomer nanocomposites.

Nanographite loading (phr)	R_B (ohm)
2	4×10^7
4	2.9×10^7
6	2.5×10^7
8	1.5×10^7

R_B: bulk resistance.

loading in the composite has a sizable effect on the dielectric properties of this system at all frequencies. From the figure it can also be observed that irrespective of the nanographite loadings, the plots yield good semicircles indicating the occurrence of polarization with a single relaxation time taking place, that is, a local mode process dominated.[19] Several attempts have been made to interpret the impedance spectroscopy of polymer–filler systems using the resistance–capacitance parallel circuit (RC) model. In a Nyquist plot for a polymer composite system, the real axis represents bulk resistivity (R_B) and the imaginary axis represents ω_{max} which is given by

$$\omega_{max} = \frac{1}{R_B C_B} \tag{8}$$

where C_B is the bulk capacitance of the polymer composite. In a Nyquist plot, increase in R_B represents poor conductivity. Figure 12 shows that with increase in nanographite loading, R_B value (in x axis) decreases or in other words, the composites become more capacitive in nature, which are calculated from the intercept of the semicircular arc on the Z' axis in Nyquist plot and tabulated in Table 3. With increasing filler loading the distance between the aggregates reduces. Each filler aggregate has a resistance (R_a), the resistance within the aggregate. The impedance in a polymer composite can be written as:

$$Z = R_{as} + \frac{R_{cs}}{1 + \omega^2 R_{cs}^2 C_s^2} - j\frac{\omega R_{cs}^2 C_s}{1 + \omega^2 R_{cs}^2 C_s^2} \tag{9}$$

The respective imaginary and real parts of impedance can be expresses as:

$$Z' = R_{as} + \frac{R_{cs}}{1 + \omega^2 R_{cs}^2 C_s^2} \text{ and } Z'' = \frac{\omega R_{cs}^2 C_s}{1 + \omega^2 R_{cs}^2 C_s^2} \tag{10}$$

The dielectric loss tangent can be expressed as:

$$\tan \partial = \frac{Z''}{Z'} = -\frac{\omega R_{cs}^2 C_s}{R_{as} + R_{cs} + \omega^2 R_{cs}^2 R_{as} C_s^2} \tag{11}$$

From the above equations the relationship between Z' and Z'' is

$$\left(Z' - \frac{2R_{as} + R_{cs}}{2}\right)^2 + Z'' = \left(\frac{R_{cs}}{2}\right)^2 \tag{12}$$

Therefore, a plot of Z'' and Z' will give a half circle which has the center at $[(2R_{as}+R_{cs})/2, 0]$ and radius of $R_{cs}/2$. Wang et al.[20] proposed that since the circular curve of the Z'' versus Z' occurs only for the parallel resistor circuit, the above analysis can be used to confirm the existence of the capacitor effect. The capacitor effect also confirms that the gap between the nanographite controls the electron conduction via non-ohmic contacts between the filler aggregates. The variation in the values of radius and center of the half circle can also be used as a measure of the gaps in between filler aggregates. It can be observed that increasing filler loadings reduces the radius and the center shifts to lower values; it can also be observed that with increasing nanographite concentrations the area under the curve in the Nyquist plot is decreasing. The intensity of this decrease is more pronounced at higher loadings of filler when compared with lower loadings. This can be explained on the basis of 'space–charge' phenomenon in heterogeneous systems. Filled rubbers are multicomponent systems that have complex molecular, supramolecular, and topological structures, which determine their ultimate properties. These structures are formed during compounding and processing. The sample preparation of rubber involves operations such as compression, cutting, and friction, which cause electrical polarization that leads to the formation of the so called mechanoelectrets.[21] The lifetime of the polarization charge depends on the polymer nature and the conditions of electrets storage and usage (temperature, dielectric characteristics of the polymer, fillers, etc.). This electrets state of rubbers has been studied in detail (especially the arising of the electrets state during processing) by Pinchuk who proposed that nonconductive rubber when subjected to high shear stresses could lead to electrets formation. These radicals could participate in polarization following several mechanisms: dipolar (directed orientation of molecules), ionic (orientation of quasi-dipoles created by weakly bonded ions) and bulk (radicals displacement to macrodistance). Increasing filler loadings lead to increased formation of more electrets thereby giving rise to more polarization. A similar explanation has been given by Leyva et al.[22] who reported the medium frequency relaxation in carbon black-reinforced polymers.

Dielectric permittivity

Figure 13 represents the variation in dielectric permittivity as a function of frequency for different concentration of nanographite-reinforced cholorobutyl elastomer composites. At fixed frequencies, the dielectric permittivity increases slowly with increasing nanographite concentrations that can be attributed to the dipoles getting less time to orient themselves in the (ever changing) direction of the alternating field. Knite et al.[23] explained the variation in dielectric permittivity as a function of

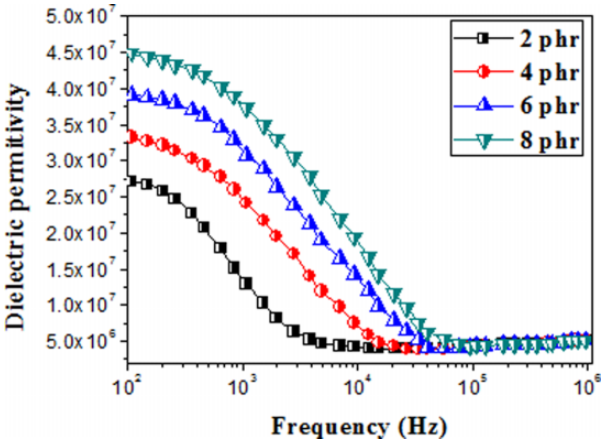

Figure 13. Dielectric permittivity as a function of frequency of chlorobutyl elastomer nanocomposites: effect of nanographite loadings.

frequency in terms of "giant tensoresistance effect." Irrespective of the fillers used in the polymer matrix, a continuous insulator–conductor transition is observed with gradual increase in the number of randomly dispersed conductor particles in the insulating polymer matrix. The volume concentration (V_c) of conductor particles at which this transition occurs is called as percolation threshold or the critical point. According to percolation theory, in the vicinity of critical concentration of filler, V_c, the variation in dielectric constant with filler concentration is given by the generalized scaling law:

$$\varepsilon \sim |V - V_c|^{-\nu}, \text{at critical point} \quad (13)$$

In agreement with the general scaling principle of the percolation theory, the relative dielectric permittivity of a two-component system (like composite) at low AC frequencies,[24] approaching the percolation threshold from both sides, diverges as:

$$\varepsilon \sim |V - V_c|^{-s},\ V < V_c \text{ or } V > V_c \quad (14)$$

In the vicinity of the percolation threshold, conductivity of the composite changes as:

$$\sigma \sim |V - V_c|^{t} \text{ for } V > V_c \quad (15)$$

and

$$\sigma \sim |V - V_c|^{-q} \text{ for } V < V_c \quad (16)$$

The power indices s, t, and q in the above equations are called as the critical indices of the percolation phase transition. In the vicinity of percolation, Wilkinson et al.[25] gave some fundamental expressions for dielectric permittivity (ε) as a function of applied frequency (f) by assuming a random distribution of conductor particles in a well-insulating matrix and modeling the composite as a network of randomly distributed capacitors.

$$\sigma \sim f^{x} \text{ and } \varepsilon \sim f^{-y} \quad (17)$$

The critical indices x and y are related by the general scaling law: $x + y = 1$.The scaling law is based on the two theoretical considerations: (a) polarization of the filler particulates within the insulating matrix (the intercluster polarization theory of Wilkinson and Langer based on classic Maxwell model) and (b) anomalous diffusion of charge carriers within the secondary filler aggregate structures (based on Aharony model of anomalous diffusion).

In case of three-dimensional composites under the assumption of body centered cubic lattice structure, theoretically the values of x and y are 0.75 and 0.29, respectively, and in face centered cubic lattice, the values are 0.68 and 0.45. But generally the structure of polymer composites is indeterminate. It depends on wide range of factors like type of filler, its dispersion within the polymer matrix, the interparticle attraction between the filler aggregates, the level of interaction between the polymer matrix and filler particulates (the well-known bound rubber phenomenon), and so on. So, the only way of obtaining the values of x and y is by semiempirical methods, in which the observed experimental data are fitted to equations. The values of x and y also provide information regarding the electrodynamics processes within the composite.

Complex dielectric modulus

Electrical response of the samples can be analyzed in terms of complex dielectric modulus formalism, which provides an alternative approach based on polarization analysis. Complex impedance spectrum gives more emphasis to elements with the largest resistance, whereas complex dielectric modulus plots highlight with smallest capacitance. Using the complex dielectric formalism, the inhomogeneous nature can be probed into bulk and grain boundary effects, which may not be distinguished from complex impedance plots. The other advantage of the dielectric modulus formalism is that the electrode effect can be suppressed. The complex dielectric modulus (M^*) have been calculated from the dielectric parameters like ε' and ε'' using the following relations:

$$M^* = \frac{1}{\varepsilon^*} = \frac{1}{\varepsilon' - i\varepsilon''} = \frac{\varepsilon'}{(\varepsilon')^2 + (\varepsilon'')^2} + i\frac{\varepsilon''}{(\varepsilon')^2 + (\varepsilon'')^2} = M' + iM'' \quad (18)$$

Where M' is real part and M'' is imaginary part of complex electric modulus and $i = \sqrt{-1}$. Based on the above equation, the dielectric data can be represented as $M'(\omega)$ and $M''(\omega)$ instead of $\varepsilon'(\omega)$ and $\varepsilon''(\omega)$ respectively, where ω is angular frequency, that is, $2\pi f$ and f is measured frequency in hertz.

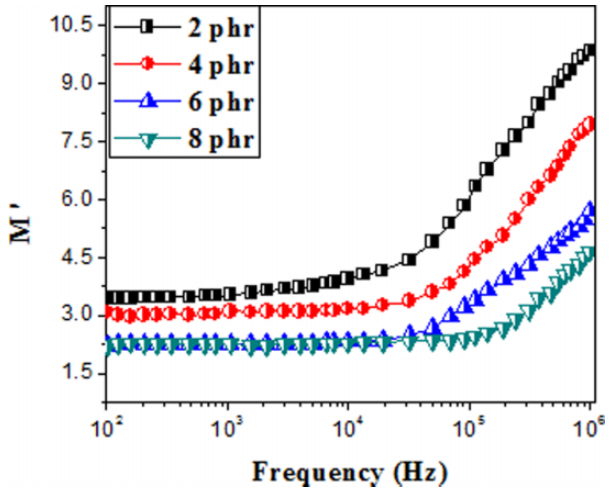

Figure 14. M' as a function of frequency of chlorobutyl elastomer nanocomposites: effect of nanographite loadings. M': real part of dielectric modulus.

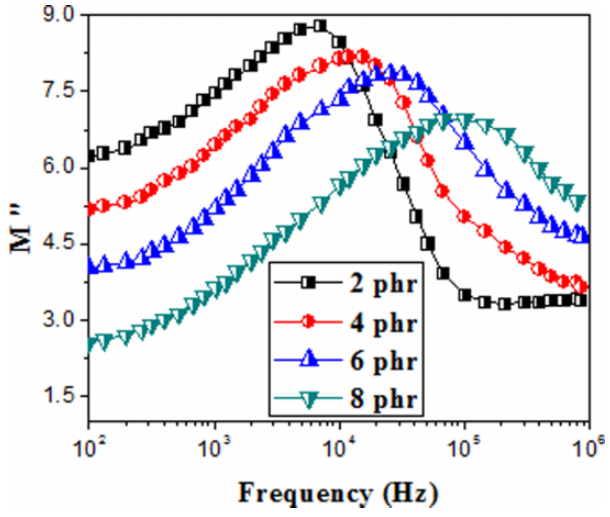

Figure 15. M'' as a function of frequency of chlorobutyl elastomer nanocomposites: effect of nanographite loadings. M'': imaginary part of dielectric modulus.

Real part of M′. Figure 14 shows variation of real part of M' as a function of frequency. A gradual increase in real part of M' with frequency is observed for all nanographite loadings. It is characterized by a very low value M' in the low-frequency region. A continuous dispersion with increase in frequency has a tendency to saturate at a maximum asymptotic value in the high-frequency region for all nanographite loadings. Such observations may possibly be related to a lack of restoring force governing the mobility of charge carriers under the action of an induced electric field. This behavior supports long-range mobility of charge carriers. Further, a sigmoidal increase in the value of M' with increasing frequency approaching ultimately maximum value may be attributed to the conduction phenomenon due to short-range mobility of charge carriers. From Figure 14, it can also be observed that with increasing nanographite loading there is a decrease in modulus values. This may be due to agglomeration of nanographite particles in the polymer matrix and the increase in interaction between the filler and polymer matrix.

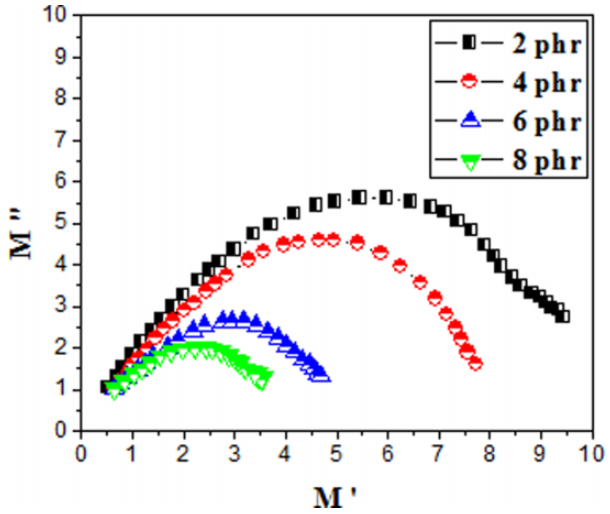

Figure 16. Argand plots of chlorobutyl elastomer nanocomposites: effect of nanographite loadings.

Imaginary part of M″. Figure 15 shows the variation of M'' with frequency at different nanographite loadings. In the accessible frequency range, the spectrum exhibits one relaxation peak for each nanographite loading. The peaks shift systematically toward higher frequencies with increase in nanographite loading for 2, 4, 6, and 8 phr, respectively. The broadening of the peak indicates the spread of relaxation time with different (mean) time constants, and hence a non-Debye type of relaxation in the materials is observed. This is very much consistent with the impedance data. The nature of the processes is further explored using the Argand diagram (complex plane representation) for dielectric modulus as shown in Figure 16 for different concentrations of nanographite loading.

Argand diagram. Figure 16 shows the relationship between M' and M'' of dielectric modulus, the so-called Argand diagram for different concentration of nanographite loadings. A semicircular trend (a requirement for non-Debye model) followed by a linear increase is observed for all nanographite loadings. It is also observed that with increase in nanographite loading the size of the semicircular loop decreases, which confirms better conduction. So, the presence of a non-Debye type of relaxations has been confirmed by complex dielectric modulus analysis.

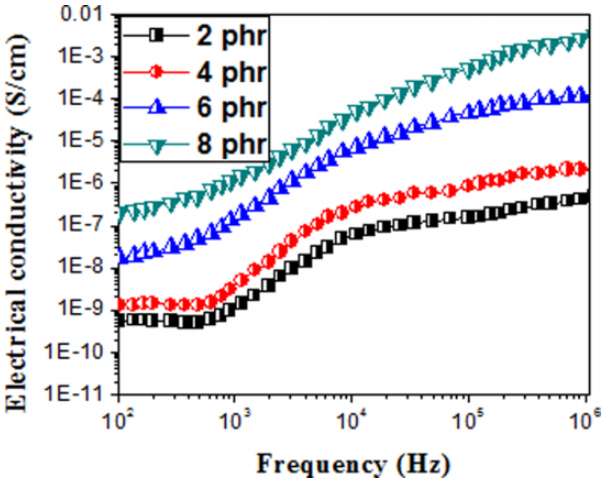

Figure 17. Variation of electrical conductivity as a function of frequency in chlorobutyl elastomer nanocomposites: effect of nanographite loadings.

Electrical conductivity

Figure 17 shows the variation of electrical conductivity with frequency at different concentration of nanographite loadings in chlorobutyl elastomer nanocomposites. Figure 17 shows the increase of electrical conductivity with frequency for all CIIR nanocomposites, at increasing nanographite concentration. The figure shows three different regions: frequency independent region (region 1), exponential growth with increasing frequency (region 2), and finally a plateau region (region 3). The shift from region 1 to region 2 depends on the nanographite concentration. In fact in 8 phr composites, region 1 is completely absent. It is widely believed that electrical properties of reinforced polymers depend primarily on the way the filler particles are distributed through the polymer matrix which is also called the mesostructure.[26] At low levels of filler loading, the conductivity of the composite is slightly higher than that of the base polymer, since the filler particles are isolated from each other by the insulating polymer matrix. When the loading of filler is low, the conductivity between the grains of filler is expected to be primarily via hopping and tunneling mechanisms. In this mode of conduction, the electron transport may be coupled strongly with the molecular and ionic processes in the insulating polymer matrix. Usually, hopping transport between localized sites is the main reason for the frequency dependence of conductivity in polymer composites. The dispersion of filler is heterogeneous, localized, and disordered. This disorder results in a wide distribution of hopping rates, giving a strong dispersion of the AC conductivity.[27,28] Hence, conductivity increases with filler loading.[29] In most of the polymer composites, a power law dependence of conductivity (σ) is observed with the variation in frequency (ω), which is represented mathematically by

Table 4. Variation of *A* and *s* with nanographite loading in chlorobutyl elastomer nanocomposites.

Nanographite loading (phr)	*A*	*s*
2	44.31	0.28
4	54.15	0.40
6	60.39	0.46
8	64.56	0.48

A: constant; *s*: exponential parameter.

$$\sigma_{AC}(\omega) \propto \omega^s \text{ or } \sigma_{AC}(\omega) = A\omega^s \quad (19)$$

where A is a constant, and s is the value of the exponential parameter, which ranges from $0 < s \leq 1$, but mostly the value is approximately $s = 1$. The frequency dependence of conductivity usually a small DC conductivity to a high localized one (at increasing frequencies) and is attributed to the polarization of the increasingly small conducting units. In disordered materials, electron transport relevant mechanisms are electron localization with associated hopping and fractal topology. According to Jonscher, the electrical conductivity of many disordered solids (including polymer composites) was found to be sum of DC conductivity (independent of frequency) and AC conductivity (strongly frequency dependent).[30] It was noted that the overall frequency dependence of conductivity (the so-called "universal dynamic response" of electron conductivity) could be approximated by the following simple relation:

$$\sigma = \sigma_{DC} + \sigma_{AC} \quad \text{or} \quad \sigma = \sigma_{DC} + A\omega^s \quad (20)$$

where $\omega = 2\pi f$ is the angular frequency, A is constant, and s is exponential parameter. For a polymer composite containing moderate concentration of filler, $s = 0.5$–0.6, and both σ and A follow strong dependencies on a variety of factors including the filler loading and temperature. The values of A and s are calculated for increasing nanographite loading and is shown in Table 4. From Table 1, it can be observed that the value of both A and s increases on increasing nanographite concentration, but the intensity of this increase is less at higher loadings of nanographite which indicates the occurrence of percolation due to the formation of continuous filler network. Figure 18 shows variation of electrical conductivity with frequency in 4 phr nanographite-reinforced chlorobutyl elastomer nanocomposite at different temperatures (i.e. 50°, 75°, and 100°C). From the figure it is clearly observed that electrical conductivity increases with increase in temperature for all nanographite loading, which confirms the negative temperature co-efficient of resistance or positive temperature co-efficient of conductivity. The increase in σ_{AC} with rise in temperature is mainly due to two phenomena:

(a) Thermal activation, which included the flocculation of particulate filler, leading to the formation of further conductive networks,

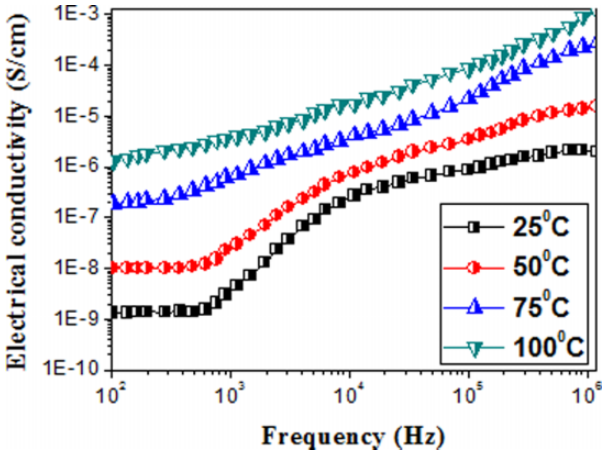

Figure 18. Variation of electrical conductivity as a function of frequency in 4 phr nanographite-reinforced chlorobutyl elastomer nanocomposites: effect of nanographite loadings.

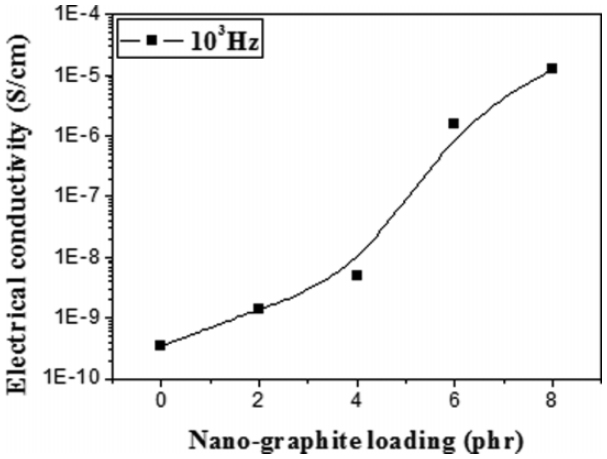

Figure 20. Variation of electrical conductivity as a function of nanographite loading in chlorobutyl elastomer nanocomposites at 10^3 Hz frequency.

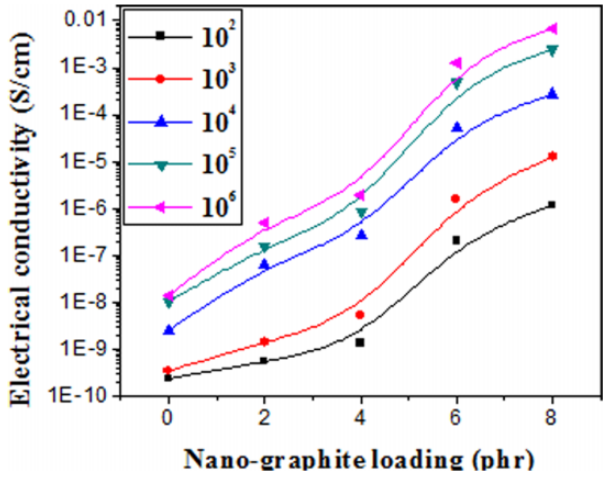

Figure 19. Variation of electrical conductivity as a function of nanographite loading at different frequency (in hertz) in chlorobutyl elastomer nanocomposites.

(b) Heating results an aerial oxidation process within the polymer matrix in the presence of nanographite that forms polar carbonyl groups.

Percolation

The variation of electrical conductivity with increasing nanographite loadings at various frequencies (10^2,10^3,10^4,10^5, and 10^6 Hz*)* is shown in Figure 19. It can be observed that irrespective of the frequency, all the samples show an abrupt increase in conductivity after 4 phr followed by a small plateau at 6 phr loading of nanographite. The electrical conductivity of a composite is generally characterized by its dependence on filler volume fraction. As the filler amount in the composite is increased, the filler particles begin to contact each other and a continuous path is formed through the volume of the sample for electrons to travel. The formation of this conductive network is based on the principles of percolation theory. Figure 20 also shows the effect of nanographite loading on the conductivity of chlorobutyl elastomer nanocomposites at 10^3 Hz frequency. Interpretation of dielectric and conductivity performance of such materials has been analyzed through percolation theory.[31] Nanda and Tripathy in their review on electrical conduction in carbon black-reinforced composites explained that percolation is due to tunneling of electrons and the conductivity is controlled by the gaps between the carbon black aggregates.[32] As the filler loading increases the nanographite sheets eventually form agglomerates. The electrical conductance in these type of heterogeneous polymer composites depend on the distance between the aggregates, hence composites can be regarded as the system composed of random arrays of closely spaced conductors dispersed in an insulating polymer matrix. Experimental results for composites consisting of an insulating matrix and conductive filler particles are often analyzed in terms of statistical percolation theory. Beyond a critical concentration of the filler, known as the percolation threshold, an increase in the composite conductivity of several orders of magnitude is observed. The theoretical value of the percolation threshold for randomly dispersed, hard, spherical particles has been determined to be about 16 vol%.[33] Percolation limit of the nanographite in this study seems to occur between 4 phr and 6 phr nanographite loading.

Conclusions

Dynamic mechanical relaxation of the nanocomposite shows that the addition of nanographite has no significant effect on the T_g. However, on increasing nanographite loadings the intensity of tan δ curve decreases. The study also shows increase in ε' values and decrease in tan δ spectra

with nanographite loadings, due to the formation of filler network. The complete semicircular Cole–Cole plots confirm the nonlinear/non-Debye type of relaxation in CIIR nanocomposite. Irrespective of nanographite loadings, smoothness of the curve indicates good dispersion of nanographite in chlorobutyl matrix. Broadening of the relaxation region was observed in the plots of ε' and ε'' values with temperature. Dielectric relaxation shows decrease in dielectric tan δ with increase in nanographite loadings. Irrespective of nanographite loading in the composite a decrease in real part of impedance with increasing frequencies has been observed, which was indicative of the capacitance nature of the composites. The variation of complex part of impedance with applied frequency shows a distinct peak. Dielectric permittivity increases slowly with increasing nanographite concentration. The real part of dielectric modulus increases with frequency and imaginary part shows a separate peak for each formulation. Electrical conductivity of CIIR nanocomposites increases exponentially with frequency and nanographite loading. The percolation threshold of the nanographite in the CIIR matrix has been studied by electrical conductivity measurements. It has been observed that the percolation limit was occurring in between 4 phr and 6 phr nanographite loading.

Funding

This research received no specific grant from any funding agency in the public, commercial or not-for-profit sectors.

References

1. Mac Farland EW and Weinberg WH. Combinatorial approaches to materials design. *TIBTECH* 1999; **17**: 107–115.
2. Gilomini Thostenson ET, Ren Z and Chou TW. Advances in the science and technology of carbon nano tubes and their composites. A review. *Compos Sci Tech* 2001; **61**: 1899–1912.
3. Psarras GC, Manolakaki E and Tsangaris GM. Electrical relaxation in polymeric particulate composites of epoxy resin and metal particles. *Compos A: Appl Sci Manuf* 2002; **33**: 375–384.
4. Das NC, Khastagir D and Chaki TK. Effect of filler treatment and crosslinking on mechanical and dynamic mechanical properties and electrical conductivity of carbon black-filled ethylene–vinyl acetate copolymer composites. *J Appl Polym Sci* 2003; **90**: 2073–2082.
5. Brosseau C, Molinie P, Boulic F, et al. Mesostructure, electron paramagnetic resonance, and magnetic properties of polymer carbon black composites. *J Appl Phys* 2001; **89**: 8297–8310.
6. Sridhar V, Chaudhary RNP and Tripathy DK. Effect of fillers on the relaxation behavior of chlorobutyl vulcanizates. *J Appl Polym Sci* 2006; **100**: 3161–3173.
7. Tiwari SK, Choudhary RNP and Mahapatra SP. Relaxation behavior of chlorobutyl elastomer nanocomposites: effect of temperature, multiwalled carbon nanotube and frequency. *J Polym Res* 2013; **20**: 176.
8. Chen G, Wu C, Weng W, et al. Preparation of polystyrene/nanosheet composites. *Polymer* 2003; **44**: 1781–1784.
9. Sridhar V, Xu D, Pham T, et al. Dielectric and dynamic mechanical relaxation behavior of exfoliated graphite reinforced flouroelastomer nanocomposites. *Polymer Compos* 2009; **111**: 1358–1368.
10. Long D and Lequeux F. Heterogeneous dynamics at the glass transition in vander waals liquids, in the bulk and in thin films. *Eur Phys J E* 2001; **4**: 371–338.
11. Ediger MD. Spatially heterogeneous dynamics in supercooled liquids. *Annu Rev Phys Chem* 2000; **51**: 99–128.
12. Trakulsujaritchok T and Hourston DJ. Damping characteristics and mechanical properties of silica filled Pur/PEMA simultaneous interpenetrating polymer net-works. *Eur Polymer J* 2006; **42**: 2968–2976.
13. Li J and Kim JK. Percolation threshold of conducting polymer composites containing 3D randomly distributed graphite nanoplatelets. *Compos Sci Technol* 2007; **67**: 2114–2120.
14. Valentini L, Amentano I, Biagotti J, et al. Frequency dependent electrical transport between conjugated polymer and single-walled carbon nanotubes. *Diamond Relat Mater* 2003; **12**: 1601–1609.
15. Huber G and Vilgis TA. On the mechanisms of hydrodynamics reinforcement in elastic composites. *Macromolecules* 2002; **35**: 9204–9210.
16. Kluppel M and Heinrich G. Fractal structures in carbon black reinforced rubber. *Rubber Chem Technol* 1995; **68**: 623–651.
17. Sridhar V, Gupta BR and Tripathy DK. Bound rubber in chlorobutyl compounds: influence of filler type and storage time. *J Appl Polym Sci* 2006; **102**: 715–720.
18. Mc-Crum NG, Read BE and Williams G. *Anelastic and dielectric effects in polymeric solids. Dover edition*. New York: Dover Inc, 1991.
19. Jawad SA and Alnajjar A. Frequency and temperature dependence of ac electrical properties of graphitized carbon black filled rubber. *Polym Int* 1997; **44**: 208–212.
20. Wang YJ, Pan Y, Zhang XW, et al. Impedance spectra of carbon black filled high density polyethylene composites. *J App Polym Sci* 2005; **98**: 1344–1350.
21. Kestelman V, Pinchuk L and Goldade V. *Electrets in engineering: fundamentals and applications*. Boston: Kluwer Academic Publishers 2000.
22. Leyva ME, Barra GMO, Moreira ACF, et al. Electric, dielectric, and dynamic mechanical behavior of carbon black/styrene-butadiene-styrene composites. *Polym Sci B: Polym Phys* 2003; **41**: 2983–2997.
23. Knite M, Teteris V, Kiploka A, et al. Reversible tenso-resistance and piezo-resistance effects in conductive polymer-carbon nanocomposites. *Adv Eng Mater* 2004; **6**: 742–746.
24. Sau KP, Chaki TK and Khastgir D. Electrical and mechanical properties of conducting carbon black filled composites based on rubber and rubber blends. *J Appl Polym Sci* 1999; **71**: 887–895.

25. Wilkinson D, Langer JS and Sen PN. Enhancement of the dielectric constant near a percolation threshold. *Phys Rev B* 1983; **28**: 1081–1087.
26. Sahoo BP, Naskar K and Tripathy DK. Conductive carbon black-filled ethylene acrylic elastomer vulcanizates: physico-mechanical, thermal, and electrical properties. *J Mater Sci* 2012; **47**: 2421–2433.
27. Ghosh P and Chakrabarti A. Conducting carbon black filled EPDM vulcanizates: assessment of dependence of physical and mechanical properties and conducting character on variation of filler loadin. *Eur Polymer J* 2000; **36**: 1043–1054.
28. Mahapatra SP, Sridhar V, Chaudhary RNP, et al. AC conductivity and positive temperature coefficient effect in microcellular EPDM vulcanizates. *Polym Compos* 2008; **29**: 1125–1136.
29. Knite V, Teteris A, Kiploka I, et al. Reversible tenso-resistance and piezo-resistance, effects in conductive polymer-carbon nanocomposites. *Adv Eng Mater* 2004; **6**: 742–746.
30. Jonscher AK. The universal dielectric Response. *Nature* 1977; **267**: 673–679.
31. Lux F. Models proposed to explain the electrical conductivity of mixtures made of conductive and insulating materirals. *J Mater Sci* 1993; **28**: 285–301.
32. Nanda M and Tripathy DK. Physico-mechanical and electrical properties of conductive carbon black reinforced chlorosulfonated polyethylene vulcanizates. *eXPRESS Polym Lett* 2008; **2**: 855–865.
33. Kim BW, Pfeifer S, Park SH, et al. The experimental determination of the onset of electrical and thermal conductivity percolation thresholds in carbon nanotube-polymer composites. *Mater Res Soc Symp Proc* 2011; **1312**: 281–286.